Biomedical Signal Processing and Control 80 (2023) 104275

Contents lists available at ScienceDirect

Biomedical Signal Processing and Control

journal homepage: www.elsevier.com/locate/bspc

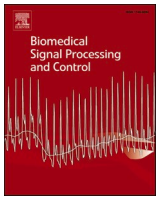

Local Pattern Transformation-Based convolutional neural network for sleep stage scoring

Hasan Zan [a,*], Abdulnasır Yildiz [b]

[a] Vocational School, Mardin Artuklu University, Mardin, Turkey
[b] Department of Electrical and Electronics Engineering, Dicle University, Diyarbakir, Turkey

ARTICLE INFO

Keywords:
Sleep stage scoring
Local pattern Transformation
LPT
One-dimensional Local Binary Pattern
1D-LBP
Local Neighbor Descriptive Pattern
LNDP
Local Gradient Pattern
LGP
Local Neighbor Gradient Pattern
LNGP
Convolutional neural network
CNN

ABSTRACT

Sleep stage scoring is essential for the diagnosis and treatment of sleep disorders. However, manual sleep scoring is a tedious, time-consuming, and subjective task. Therefore, this paper proposes a novel framework based on local pattern transformation (LPT) methods and convolutional neural networks for automatic sleep stage scoring. Unlike in previous works in other fields, these methods were not employed for manual feature extraction, which requires expert knowledge and the pipeline behind it might bias results. The transformed signals were directly fed into a CNN model (called EpochNet) that can accept multiple successive epochs. The model learns features from multiple input epochs and considers inter-epoch context during classification. To evaluate and validate the effectiveness of the proposed approach, we conducted several experiments on the Sleep-EDF dataset. Four LPT methods, including One-dimensional Local Binary Pattern (1D-LBP), Local Neighbor Descriptive Pattern (LNDP), Local Gradient Pattern (LGP), and Local Neighbor Gradient Pattern (LNGP), and different polysomnography (PSG) signals were analyzed as sequence length (number of input epochs) increased from one to five. 1D-LBP and LNDP achieved similar performances, outperforming other LPT methods that are less sensitive to local variations. The best performance was achieved when an input sequence containing five epochs of PSG signals transformed by 1D-LBP was employed. The best accuracy, F1 score, and Kohen's kappa coefficient were 0.848, 0.782, and 0.790, respectively. The results showed that our approach can achieve comparable performance to other state-of-the-art methods while occupying fewer computing resources because of the compact size of EpochNet.

1. Introduction

Sleep, being one of the most basic biological functions, is essential for both physical and mental well-being [1]. Sleep disorders such as sleep apnea, insomnia, and restless legs syndrome can cause shortened sleep by disrupting sleep or preventing the patient from sleeping [2]. Sleep deprivation can result in emotional, cognitive, and physiological complications such as depressed mood, exhaustion, reduced decision-making, cardiovascular disease, an increased risk of cancer, and diabetes [3]. Accordingly, monitoring and analysis of sleep are of great importance for the assessment of sleep quality and diagnosis of sleep disorders in medicine [4]. The first step of such an analysis is sleep stage scoring or detection. The collection and analysis of physiological data during sleep is required for the diagnosis of any type of sleep disorder [5].

Traditionally, sleep stage scoring requires the use of polysomnography (PSG), which is a test that uses physiological signals such as electroencephalogram (EEG), electrooculogram (EOG), and electromyogram (EMG) [6]. The test is conducted by experts who visually inspect and analyze the whole night PSG signals, epoch by epoch (30-second segment) according to predefined rules. As per Rechtschaffen and Kales (R&K) rules, an entire night of sleep for an adult is split into six stages: wakefulness (W), non-rapid eye movement (stages 1 to 4, N1 to N4), and rapid eye movement (REM) [7]. New criteria were set by the American Academy of Sleep Medicine (AASM) in 2004, merging stages 3 and 4 into stage N3 [4]. Traditional sleep scoring requires expert knowledge and is a time-consuming task. Furthermore, it is susceptible to inter- and intra-scorer variability, causing the results of a single PSG record to differ at different times despite being conducted by the same scorer. As a result, automatic sleep stage detection has drawn a lot of interest in recent decades.

Usually, automatic sleep stage classification involves three main phases: preprocessing, feature extraction, and classification. Preprocessing comprises cleaning (noise cancellation and removing linear

* Corresponding author.
E-mail address: hasanzan@artuklu.edu.tr (H. Zan).

https://doi.org/10.1016/j.bspc.2022.104275
Received 18 May 2022; Received in revised form 13 September 2022; Accepted 26 September 2022
Available online 12 October 2022

trends), smoothing (filtering high frequencies) of data collected using PSG or other acquisition systems, and transformation of raw data as well as segmentation of processed data. Feature extraction is a set of operations that includes deriving informative and non-redundant values, commonly after signal transformations that help to reveal patterns hard to detect in the time domain. As a result, a long signal is represented by a set of values called feature vector that provides the basis for classification. These features are usually specified by the experience of specialists and can be classified into four categories: 1) time domain features that do not require any signal transformations, 2) frequency domain features that frequently use the Fourier transform, 3) time–frequency domain features that include a transformation such as the short-time Fourier, wavelet, or Hilbert-Huang, and 4) non-linear features [8]. The purpose of classification is to establish an optimal mapping from features to class labels. Various machine learning techniques, i.e., artificial neural networks [9], k-nearest neighbors [10], k-means clustering [11], support vector machines [12], decision trees [13], as well as ensemble classifiers [14–16] have been utilized for the classification of sleep stages.

Another way to perform feature extraction and classification is to use deep learning (DL), which has achieved state-of-the-art performance in many fields, including computer vision and image recognition, time series prediction, and biomedical image and signal classification [17–19]. It learns how to extract useful features directly from its input during training. Thus, it does not require manual feature extraction, which is crucial for classification performance and generally demands field expertise. As a result, DL algorithms have recently been used for sleep stage classification [20]. Researchers have commonly utilized three DL approaches: convolutional neural networks (CNNs), recurrent neural networks (RNNs), and hybrid models that contain both CNNs and RNNs. CNNs learn intra-epoch features by convolution, activation, and pooling operations from epochs, disregarding inter-epoch relations among successive epochs, while RNNs can learn inter-epoch relations. RNNs can thus be utilized in hybrid models to consider the inter-epoch relationships between epoch features obtained independently from each epoch by CNNs [21].

In addition, among DL-based sleep staging methods, two preeminent groups can be determined: methods 1) using raw PSG signals and 2) using transformed PSG signals. Sors et al. [22] utilized raw single-channel EEG signals and a CNN model with 14 layers to classify sleep stages. Chambon et al. [23] used raw PSG signals, including EEG, EMG, and EOG, as input to a CNN model consisting of 11 layers to detect different sleep stages. Seo et al. [24] proposed a method employing raw EEG signals. The method extracts spatial features using a deep residual neural network, which is a type of CNN, and learns the temporal context of extracted features using two layers of bidirectional long short-term memory (bi-LSTM), which is a type of RNN. Supratak et al. [21] used raw single-channel EEG signals and a DNN model with a CNN and an RNN to categorize sleep stages. Khalili et al. [25] employed a CNN to extract spatial features, followed by a modified CNN called temporal CNN to extract temporal features. They classified sleep stages based on single-channel raw EEG signals. In general, these types of studies have avoided the use of any signal transformations due to the lack of computationally efficient methods that do not increase the dimensionality of input signals.

Among methods that utilize transformed signals, Phan et al. [26] proposed a CNN-based joint classification and prediction method. Their innovative framework determines a single input epoch's label as well as the labels of its nearby epochs. They used log-power spectra images of PSG signals instead of raw signals to exploit frequency domain features. Dong et al. [27] employed short-time Fourier transform to generate time–frequency representations of single-channel EEG signals, which are spectrograms. In their study, generated spectrograms were fed to an RNN model to classify spectrogram images that represent epochs. Biswal et al. [28] proposed a framework containing both a CNN and an RNN to recognize sleep stages. In the framework, the CNN first extracts time-invariant features from spectrograms of 30-second epochs of EEG signals. The extracted features are then fed to the RNN to learn inter-epoch features. Hsu et al. [29] proposed an RNN-based method that classifies energy features extracted from 30-second epochs of EEG signals into different sleep stages. Jadhav et al. [30] proposed using pre-trained CNN models to classify sleep stages. They exploited time–frequency features using scalogram images generated by continuous wavelet transform (CWT) as input to CNN models. Their results showed that employing signal transformations prior to the DNN model provides additional representative context to the models and has the potential to improve the performance of sleep stage classification.

Recently, several local pattern transformation-based feature extraction techniques have been introduced [31–34]. Local pattern transformations include One-dimensional Local Binary Pattern (1D-LBP) and several methods derived from it, including Local Neighbor Descriptive Pattern (LNDP), Local Gradient Pattern (LGP), Local Neighbor Gradient Pattern (LNGP), Local Centroid Pattern (LCP), and One-Dimensional Local Ternary Pattern (1D-LTP). These techniques have been employed as signal transformations prior to the calculation of statistical or histogram features, limiting their effectiveness and increasing the risk of biased results. Furthermore, even though they have shown promising results in relatively easy tasks such as epileptic EEG classification [31,32,35,36], and detection of Parkinson's disease [33,37], further investigation is required to assess and verify their effectiveness.

This study aims to evaluate and validate a novel approach for the detection of sleep stages from PSG signals. The approach is based on the use of local pattern transformations and CNNs. PSG signals are transformed into new signals containing local patterns using one of the local pattern transformation (LPT) methods. Transformed signals are segmented into 30-second epochs. Classification has been carried out using a CNN model (called EpochNet) that can accept multiple successive epochs. The model learns features from multiple epochs and considers inter-epoch context during classification. The classification performance has been evaluated on the benchmark dataset, PhysioNet Sleep-EDF Expanded [38] using leave-one-out 20-fold cross-validation.

The summary of the study is as follows:

- To the best of our knowledge, this is the first study to apply LPT methods to sleep stage scoring. In addition, unlike in previous works in other fields, LPT was not employed for manual feature extraction. The transformed signals were directly fed into the CNN for feature extraction and classification.
- The study investigates the role of LPT methods prior to the classification. We evaluate four LPT methods: One-dimensional Local Binary Pattern (1D-LBP), Local Neighbor Descriptive Pattern (LNDP), Local Gradient Pattern (LGP), and Local Neighbor Gradient Pattern (LNGP).
- PSG, both single-channel and multi-channel, was extensively used in the analysis. We consider single- and multi-channel EEG, single-channel EOG, and combinations of both.
- A novel CNN model was employed for feature extraction and classification: EpochNet, a CNN model with a variable number of inputs and accepting one epoch for each input. Before classification, the model extracts epoch features from many subsequent epochs in parallel and blends them to construct inter-epoch links among extracted features.
- Since LPT methods transform a given signal into a certain range, the proposed approach does not require normalization or standardization of PSG signals. Furthermore, PSG signals are not filtered before the transformation, the approach relies on the discriminative power of discovered local patterns.
- The proposed approach was evaluated on the Sleep-EDF Expanded dataset, and experimental results showed that it performs on par with existing methods on the experimental dataset.

The rest of this paper is organized as follows. The dataset utilized in this study is detailed in Section 2. Section 3 describes the research

methodology by elaborating on the LPT-based strategy for sleep stage scoring that we present. Also, the CNN model structure is explained. Section 4 describes the experimental setup and gives a summary of the findings. Lastly, Sections 5 and 6 present the work's discussion and conclusion, respectively.

2. Dataset

The experimental data used in this study is the Sleep-EDF Expanded (2013 version) database supplied by Physionet, which is a widely used database in the sleep stage classification literature. This database has PSG recordings of 20 healthy subjects (sc* recordings) and 22 unhealthy subjects (st* recordings). Each recording contains two-channel EEG (Fpz-Cz and Pz-Oz) and horizontal EOG, each sampled at 100 Hz. sc* recordings include the envelope of submental EMG sampled at 1 Hz while st* recordings have submental EMG sampled at 100 Hz. The sc* recordings were collected from healthy volunteers during 24 h of daily life, and the st* recordings contain whole-night PSG signals collected from subjects with mild difficulty falling asleep but were who otherwise healthy. Each epoch of recordings was annotated by experts according to R&K rules as W, N1, N2, N3, N4, REM, Movement, or Unknown. Due to the duration of wakefulness in comparison to other classes, we used only thirty minutes before and after the sleep period [24]. In line with previous studies [20], Movement and Unknown epochs were excluded, and N3 and N4 were merged based on AASM criteria. In this study, 39 sc* recordings of 20 subjects were used for extensive analysis of the proposed method. The class-wise number of epochs in the dataset is listed in Table 1.

3. Methodology

In this section, a brief discussion about the proposed framework, local pattern transformation techniques, and the CNN model used has been done.

3.1. The framework

We propose a novel framework based on LPT and CNN for sleep stage scoring. Unlike in previous studies, LPT methods were used to transform PSG signals to capture hidden local patterns. Four LPT methods, i.e., LBP, LNDP, LGP, and LNGP, were employed to discover local patterns hidden in PSG signals. Feature extraction and classification were conducted by the CNN model directly from epochs of transformed signals. The CNN model, EpochNet, can accept multiple successive epochs of PSG signals to extract inter- and intra-epoch features. Fig. 1 illustrates the block diagram of the proposed framework.

Human sleep experts visually analyze the frequency features and sleep-related events such as K-complexes and sleep spindles when labeling each 30-second PSG epoch with its relevant sleep stage. Furthermore, they analyze sleep-related events in nearby epochs to determine whether the events' relationships adhere to the transition rules [24]. Likewise, EpochNet learns features that represent sleep-related events from discovered local patterns of epochs and detects the sleep stages of target epochs using both target and neighboring epochs.

As shown in Fig. 1, EpochNet has two main parts: branches and a classification head. The number of branches depends on the selection of the number of input epochs (N). Each branch is responsible for extracting useful information from its input epoch. A branch consists of a series of blocks, each with two convolution layers, a batch normalization, a Rectified Linear Unit (ReLu), and a max-pooling layer. Extracted features are concatenated and classified by the classification head that comprises a global average pooling, a dropout layer, and a dense layer with softmax activation. Section 3.7 details the CNN model.

EpochNet has been designed to facilitate single-epoch inputs or successive multi-epoch inputs. With single-epoch inputs ($N = 1$), it disregards any sleep-related events from previous epochs that could affect the scoring of target epochs. However, in many cases, human experts decide the stage of target epochs based on the events from both the target epochs and previous epochs. For example, an epoch where arousal is observed changes the decision regarding the stage of the epoch that follows it. Arousals cause the transition from deep sleep to light sleep or wakefulness [39]. Therefore, we used multiple successive epochs ($N > 1$) as inputs to EpochNet to establish inter-epoch relations when scoring target epochs.

Table 1
Number of epochs in the dataset.

W	N1	N2	N3	REM	Total
8284 (19.6 %)	2804 (6.6 %)	17,799 (42.1 %)	5703 (13.5 %)	7717 (18.2 %)	42,307 (100 %)

3.2. Local pattern transformation techniques

One-dimensional Local Binary Pattern (1D-LBP) has recently gained attention in the fields of EEG signal classification [31,32] and gait-based Parkinson's disease detection [33,37]. During transformation, 1D-LBP focuses on the local pattern structure of a signal and can discover these patterns [32]. Due to the sensitivity of 1D-LBP to local variations, researchers have derived several 1D-LBP-based methods that are insensitive to local variations and preserve the structural property of discovered patterns. In this section, we briefly explain 1D-LBP and methods derived from it, including LNDP, LGP, and LNGP.

3.3. One-dimensional local binary pattern

1D-LBP is a variant of Local Binary Pattern (LBP), a basic but effective texture operator used for grayscale images [40]. It captures local patterns by comparing center values with determined neighbor values. The calculation steps of 1D-LBP are as follows:

1) Set the number of neighboring points, n.
2) For each signal point S_c, determine $n/2$ neighboring points on the left and right of the point.
3) Calculate the difference between neighboring points p_i and S_c as: $d_i = p_i - S_c$, for $n = 0, 1, \cdots, n-1$.
4) Calculate the binary value for each difference d_i as:

$$b_i = \begin{cases} 0, d_i < 0 \\ 1, d_i \geq 0 \end{cases}$$

5) Convert the resultant binary number $(b_{n-1}b_{n-2}\cdots b_0)_2$ to decimal.

3.4. Local neighbor descriptive pattern

LNDP, introduced by Jaiswal and Banka [32], is an LBP-based method that captures the neighborhood relationship while preserving the pattern's structural property. The calculation steps of LNDP are as follows:

1) Set the number of neighboring points, n.
2) For each signal point S_c, determine $n/2$ neighboring points on the left and right of the point.
3) Calculate the difference between consecutive points p_i as: $d_i = p_i - p_{i+1}$, for $n = 0, 1, \cdots, n-1$.
4) Calculate the binary value for each difference d_i as:

$$b_i = \begin{cases} 0, d_i < 0 \\ 1, d_i \geq 0 \end{cases}$$

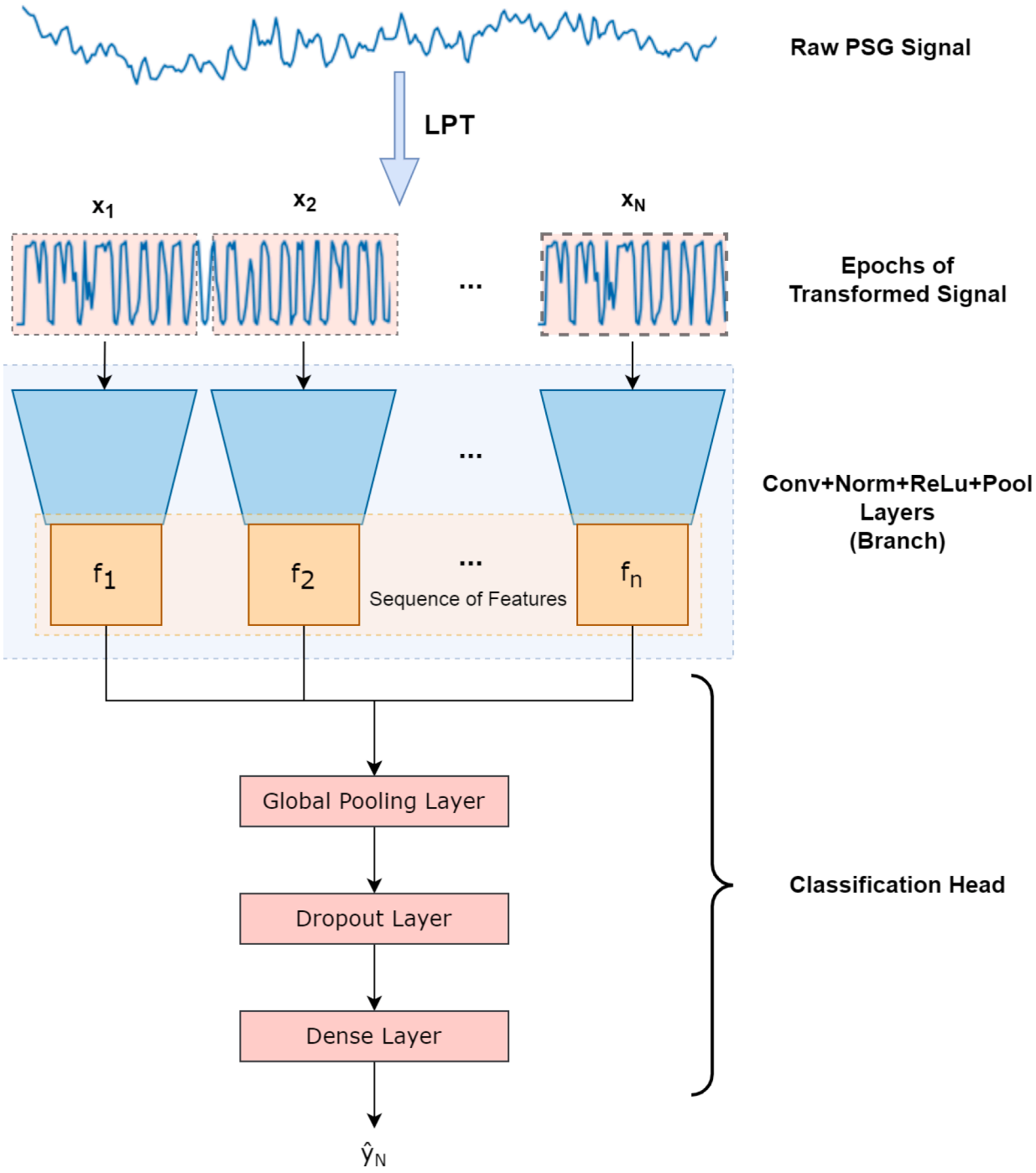

Fig. 1. Block diagram of the LPT-based framework.

5) Calculate the resultant binary number $(b_{n-1}b_{n-2}\cdots b_0)_2$ to decimal.

3.5. Local gradient pattern

LGP captures global variations along with certain local dissimilarities [32]. This method also preserves the structural property of a pattern. The calculation steps of LGP are as follows:

1) Set the number of neighboring points, n.
2) For each signal point S_c, determine $n/2$ neighboring points on the left and right of the point.
3) Calculate the gradient between neighboring points p_i and S_c as: $g_i = |p_i - S_c|$, for $n = 0, 1, \cdots, n-1$.
4) Calculate mean gradient g_m by averaging gradients g_i.
5) Calculate the difference between gradients and mean gradient as: $d_i = g_i - g_m$, for $n = 0, 1, \cdots, n-1$.
6) Calculate the binary value for each difference d_i as:

$$b_i = \begin{cases} 0, d_i < 0 \\ 1, d_i \geq 0 \end{cases}$$

7) Convert resultant binary number $(b_{n-1}b_{n-2}\cdots b_0)_2$ to decimal.

3.6. Local neighbor gradient pattern

LNGP compares consecutive gradient points in order to eliminate

noise-induced local and global pattern fluctuations [34]. This method also preserves the structural property of a pattern. The calculation steps of LNGP are as follows:

1) Set the number of neighboring points, n.
2) For each signal point S_c, determine $n/2$ neighboring points on the left and right of the point.
3) Calculate the gradient between neighboring points p_i and S_c as: $g_i = |p_i - S_c|$, for $n = 0, 1, \cdots, n-1$.
4) Calculate the difference between consecutive gradients as: $d_i = g_i - g_{i+1}$, for $n = 0, 1, \cdots, n-1$.
5) Calculate the binary value for each difference d_i as:

$$b_i(d_i) = \begin{cases} 0, d_i < 0 \\ 1, d_i \geq 0 \end{cases}$$

6) Convert the resultant binary number $(b_{n-1}b_{n-2}\cdots b_0)_2$ to decimal.

We set the number of neighboring points, n to eight for all methods. Fig. 2 and Fig. 3 depict segments of sample EEG and EOG signals and signals transformed by 1D-LBP, LNDP, LGP, and LNGP. It can be seen that LPT methods transform any real-valued signal into a new integer-valued signal in the range of [0, 255], which is a newly discovered pattern. A comparative analysis regarding discovered patterns can be found in Ref. [32].

3.7. Model structure

EpochNet is designed to accept single or multiple successive epochs transformed by the LPT. Depending on the number of epochs, a branch or multiple branches extract useful features from inputs. Each branch consists of five blocks, and each block has five layers. Table 2 details the blocks and layers in each branch. The branch structure was determined through our prior knowledge and initial experiments. Initial experiments were used to determine the number of blocks and filters by observing model fit during training. Model capacity, i.e., the number of blocks and filters, was increased or decreased based on training progress. A simple structure that can provide both high training speed and accuracy is formed. Two convolution layers with different filter sizes are used in each block to capture multiscale representative features. In particular, the small filter is more likely to learn local pattern information (when a particular pattern arises during a particular sleep stage), while the large filter is better at capturing frequency information [21]. They are followed by a batch normalization layer that provides faster convergence during training. A ReLu is used for non-linearity, and a max-pooling layer is employed to reduce the dimensionality of extracted

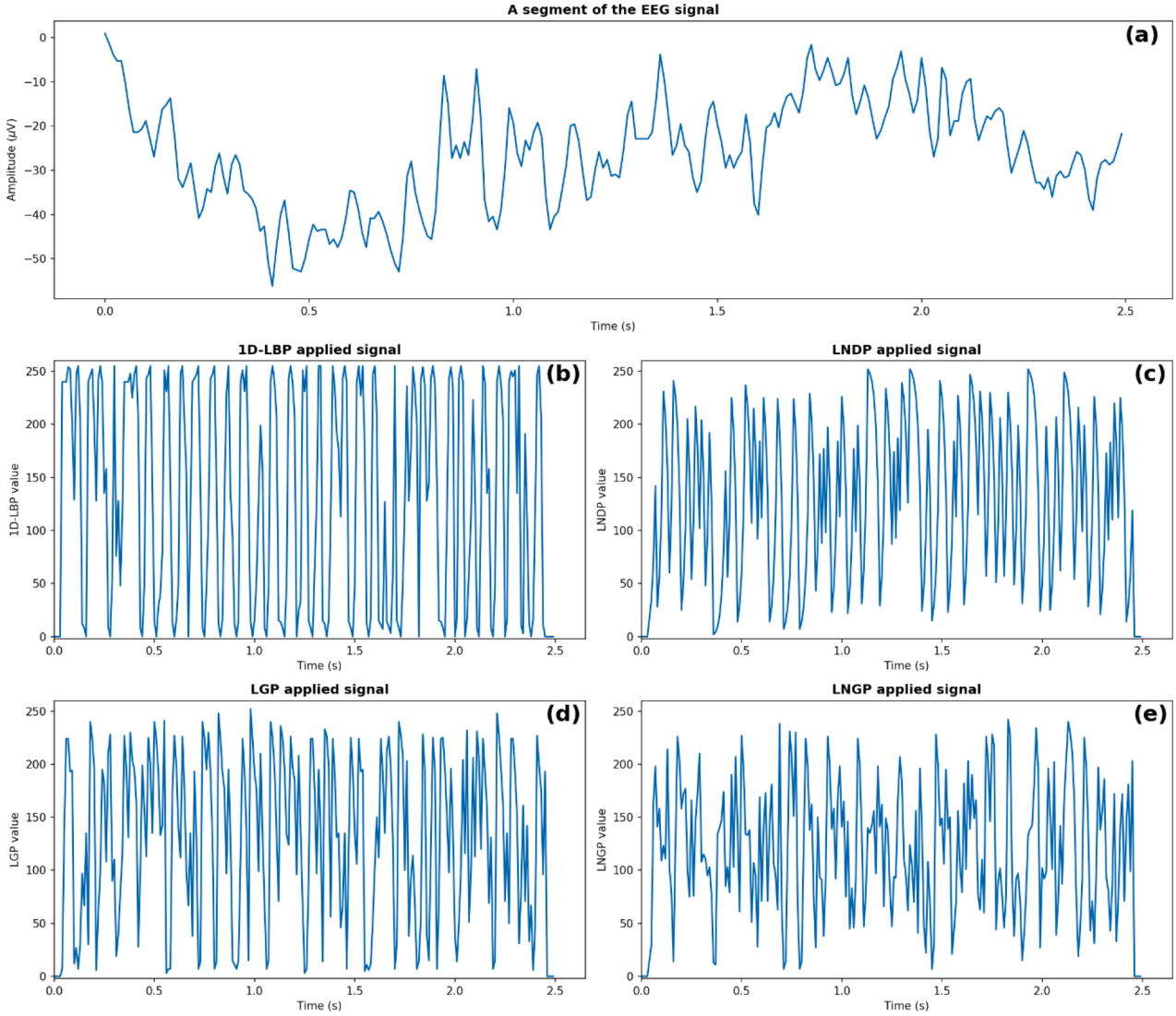

Fig. 2. (a) a segment of a sample EEG signal. The signal transformed by (a) 1D-LBP, (b) LNDP, (c) LGP, and (d) LNGP.

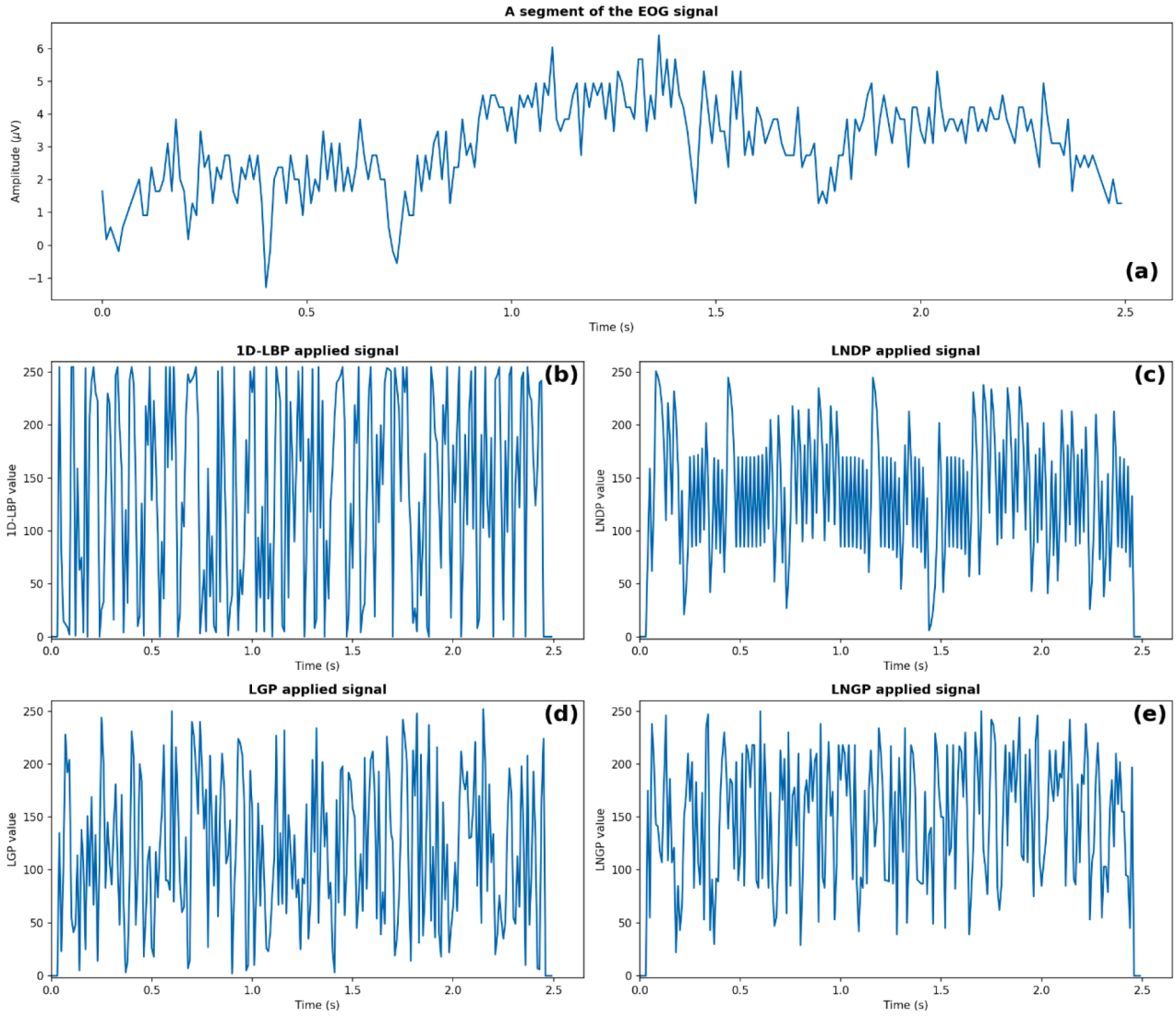

Fig. 3. (a) a segment of a sample EOG signal. The signal transformed by (a) 1D-LBP, (b) LNDP, (c) LGP, and (d) LNGP.

features. In the following blocks, we reduce the filter size of convolution layers for faster training and increase the number of filters to extract more complex features. As a result, epoch $\mathbf{x} \in \mathbb{R}^{3000\times m}$ is represented by a feature map $\mathbf{f} \in \mathbb{R}^{94\times 32}$ at the end of the branch, where m is the number of PSG signals in the epoch.

Furthermore, we replace the more traditional fully connected layer with a global average pooling layer, which has been shown to be more robust to small shifts in the input [41]. A dropout layer with a probability of 0.2 is employed to increase the generalization capability of the model. Finally, classification is done by a dense layer with softmax activation, producing label $\widehat{y}$ for the target epoch. In the case of multiple epochs, the model takes a sequence of epochs $\mathbf{X_N} = \{\mathbf{x}_1, \mathbf{x}_2, \cdots, \mathbf{x_N}\}$ and predicts the label $\widehat{y}_N$ for the target epoch, where $\mathbf{x_N}$ is the target epoch and $\mathbf{x}_1, \mathbf{x}_2, \cdots, \mathbf{x}_{N-1}$ are the previous epochs. Branch b_i extracts a feature map $\mathbf{f}_i \in \mathbb{R}^{94\times 32}$ from its input epoch $\mathbf{x_i} \in \mathbb{R}^{3000\times m}$ for $i = 1, 2, \cdots, N$. Then, along the first axis, the sequence of features $\mathbf{S_N} = \{\mathbf{f}_1, \mathbf{f}_2, \cdots, \mathbf{f_N}\}$ is concatenated, yielding a feature map $\mathbf{F_N} \in \mathbb{R}^{(N\times 94)\times 32}$, which blends features from multiple epochs. The final layer computes the label $\widehat{y}_N$ for the target epoch $\mathbf{x_N}$, taking into account both intra- and inter-epoch features.

3.8. Training

In line with previous literature [42], we followed a subject-wise Leave-One-Out Cross-Validation (LOOCV) scheme. Since there are 20 subjects in the dataset, it was divided into 20 subsets, each containing the PSG records of one subject. In each fold, training was performed on a training set consisting of 19 subsets, and the remaining was used for the test. Training and testing were repeated until all 20 subsets were used for the test. All predictions were aggregated for evaluation via the calculation of performance metrics.

The Adam optimizer [43] with the following parameters: $\beta_1 = 0.9$, $\beta_2 = 0.999$, and $\epsilon = 10^{-7}$ were employed. These parameters are default values for the optimizer in Tensorflow 2.5 [44], and they have been reported to perform well for many applications [45]. Learning rate was determined through initial experiments as $lr = 0.0001$. No strategies to balance out the unequal distribution of classes in data processing or model training were used. Early stopping was achieved by observing the validation accuracy and terminating the training after 20 consecutive training steps with no improvement in the validation accuracy. The model with the best validation accuracy was utilized for prediction in the test set for each fold of the cross-validation. The model and training progress were implemented in Python 3.8 and TensorFlow 2.5 [44].

Table 2
Parameters of each branch.

Block	Layer Type	# of Filters	Size	Stride	Output Dimension
1	Conv1D	16	11	1	(3000, m)
1	Conv1D	16	9	1	(3000, 16)
1	BatchNormalization	–	–	–	(3000, 16)
1	ReLu	–	–	–	(3000, 16)
1	MaxPooling1D	–	3	2	(1499, 16)
2	Conv1D	16	9	1	(1499, 16)
2	Conv1D	16	7	1	(1499, 16)
2	BatchNormalization	–	–	–	(1499, 16)
2	ReLu	–	–	–	(1499, 16)
2	MaxPooling1D	–	3	2	(749, 16)
3	Conv1D	32	7	1	(749, 32)
3	Conv1D	32	5	1	(749, 32)
3	BatchNormalization	–	–	–	(749, 32)
3	ReLu	–	–	–	(749, 32)
3	MaxPooling1D	–	3	2	(374, 32)
4	Conv1D	32	5	1	(374, 32)
4	Conv1D	32	3	1	(374, 32)
4	BatchNormalization	–	–	–	(374, 32)
4	ReLu	–	–	–	(374, 32)
4	MaxPooling1D	–	3	2	(186, 32)
5	Conv1D	32	5	1	(186, 32)
5	Conv1D	32	3	1	(186, 32)
5	BatchNormalization	–	–	–	(186, 32)
5	ReLu	–	–	–	(186, 32)
5	MaxPooling1D	–	3	2	(94, 32)

3.9. Evaluation

As stated in the previous section, to measure the performance of the proposed approach in different cases, a subject-wise LOOCV scheme was followed. Evaluation was done based on aggregated predictions. We used the following metrics: accuracy (*ACC*), F1 score (*F*1), and Cohen's kappa coefficient (κ). Accuracy is the ratio of the correct predictions to the total predictions, which can be misleading in the case of an imbalanced class distribution. It is defined as:

$$ACC = \frac{TP + TN}{TP + FN + TN + FP} \tag{1}$$

where *TP*, *FP*, *TN*, and *FN* stand for the numbers of true positives, false positives, true negatives, and false negative, respectively. F1 score is the harmonic mean of Precision (*PR*) and Recall (*RE*), thus, it can provide more information than accuracy. F1 score is defined as:

$$F1 = 2\frac{PR \times RE}{PR + RE} \tag{2}$$

where.

$$PR = \frac{TP}{TP + FP} \tag{3}$$

$$RE = \frac{TP}{TP + FN} \tag{4}$$

Cohen's kappa coefficient measures the agreement in sleep scoring between human experts and EpochNet. It is defined as:

$$\kappa = \frac{p_o - p_e}{1 - p_e} \tag{5}$$

where p_o is the relative observed agreement among raters, and p_e is the hypothetical probability of chance agreement.

4. Results

In this study, a novel approach based on LPT and CNN for sleep stage scoring is introduced. To the best of our knowledge, this is the first study to apply LPT methods to PSG signals and sleep scoring. Furthermore, in contrast to the previous studies that used LPT methods in other fields, the approach does not employ any manual feature extraction techniques, relying instead on the model for feature extraction. Sixty experiments were designed for extensive analysis. Experiments cover four LPT methods, three signals (Fpz-Cz EEG, Pz-Oz EEG, and horizontal EOG), two signal combinations (two-channel EEG, two-channel EEG + EOG), and three values for the number of epochs (N = 1, 3, and 5). Experiments are presented in accordance with the signal(s) used.

Table 3 lists experiments conducted using Fpz-Cz EEG, different LPT methods, and the number of epochs. Each experiment was carried out under the same setup except for the LPT method used to transform signals and the number of epochs utilized. Overall, the best accuracy, F1 score, and Cohen's kappa were 0.839, 0.762, and 0.777, respectively. The best class-wise F1 scores for W, N1, N2, N3, and REM were obtained as follows: 0.888, 0.373, 0.877, 0.843, and 0.827, respectively. In terms of LPT, regardless of the number of epochs, 1D-LBP provided the most discriminative patterns, while LGP and LNGP performed significantly worse than the others. The results also showed that models with more inputs achieved better performance.

Since studies using different methods reported opposite results for the best-performing EEG channel [21], we conducted the same experiments using the Pz-Oz channel as well. Table 4 summarizes the results obtained for this channel. In this case, overall performance slightly decreased to 0.827 for accuracy, 0.729 for F1 score, and 0.815 for kappa. 1D-LBP was still the best method, while LGP and LNGP were the worst. With the exception of 1D-LBP, models with three inputs demonstrated slightly better performance.

Even though EEG conveys the most relevant information regarding sleep stages, its collection is not the most convenient for subjects. In addition, the inconvenience it causes due to electrode placement can disturb subjects' sleep patterns. Thus, we provided performance results for horizontal EOG, considering the convenience it can provide due to electrode positioning. Table 5 compiles the outcomes of the performance evaluation using EOG. Since EOG is the secondary signal for sleep scoring and carries indirect information, using only this signal resulted in a significant decrease in the overall and per-class performance. The model accepting three successive epochs of EOG signals transformed by 1D-LBP achieved the highest accuracy (0.802), F1 score (0.721), and kappa (0.793). In addition, the performance gap among 1D-LBP and the others increased. In a few circumstances, LGP and LNDP were unable to accurately categorize even a single N1 epoch.

We conducted experiments using both EEG channels to investigate and analyze signal fusion. Regardless of the number of epochs or method used, each experiment employed epochs with a size of 3000-by-2 ($m = 2$). Table 6 shows the outcomes of these experiments. Using 1D-LBP, we achieved the best accuracy, F1 score, and kappa, reaching 0.846, 0.77, and 0.787, respectively. Apart from the LNDP, all methods achieved their best performance with N = 5. In terms of maximum accuracies, 1D-LBP, LNDP, and LGP recorded an increase in their accuracy compared to single channel EEG, while LNGP did not benefit from signal fusion.

Finally, EOG was combined with two-channel EEG to create 3000-by-3 epochs ($m = 3$) that were supplied into the models. Performance results for experiments using all signals are listed in Table 7. The best results were achieved by 1D-LBP and the model with five inputs, which improved to 0.848 accuracy, 0.782 F1 score, and 0.790 kappa. Except for LNGP, the accuracy of all LPT methods exceeded 0.80. The best per-class F1 scores were 0.912, 0.444, 0.883, 0.849, and 0.834 for W, N1, N2, N3, and REM, respectively.

5. Discussion

In this paper, we proposed a novel framework based on LPT methods and CNNs for the detection of sleep stages from PSG signals. Four LPT methods, i.e., 1D-LBP, LNDP, LGP, and LNGP, were employed to transform raw PSG signals before feature extraction and classification by CNN. The CNN model was designed to accept single or multiple successive epochs. With the use of multiple epochs, the model was able to

Table 3
Performance results for the Fpz-Cz EEG, as well as various LPT methods and the number of epochs.

N	LPT	*ACC*	*F*1	κ	Per-Class *F*1				
					W	N1	N2	N3	REM
1	1D-LBP	0.814	0.720	0.744	0.874	0.254	0.865	0.851	0.755
1	LNDP	0.800	0.690	0.721	0.871	0.179	0.854	0.823	0.723
1	LGP	0.759	0.637	0.663	0.829	0.085	0.826	0.774	0.670
1	LNGP	0.730	0.605	0.620	0.830	0.061	0.796	0.712	0.626
3	1D-LBP	0.834	0.747	0.770	0.879	0.307	0.877	0.851	0.819
3	LNDP	0.816	0.701	0.745	0.864	0.156	0.867	0.827	0.789
3	LGP	0.754	0.623	0.649	0.840	0.085	0.817	0.696	0.677
3	LNGP	0.756	0.627	0.651	0.853	0.091	0.817	0.714	0.661
5	1D-LBP	0.839	0.762	0.777	0.888	0.373	0.877	0.843	0.827
5	LNDP	0.812	0.701	0.738	0.874	0.179	0.861	0.826	0.766
5	LGP	0.775	0.663	0.684	0.834	0.145	0.836	0.793	0.706
5	LNGP	0.772	0.635	0.679	0.845	0.036	0.831	0.760	0.704

Table 4
Performance results for the Pz-Oz EEG, as well as various LPT methods and the number of epochs.

N	LPT	*ACC*	*F*1	κ	Per-Class *F*1				
					W	N1	N2	N3	REM
1	1D-LBP	0.802	0.669	0.725	0.881	0.056	0.860	0.808	0.742
1	LNDP	0.767	0.641	0.68	0.855	0.05	0.828	0.781	0.689
1	LGP	0.749	0.615	0.65	0.863	0.007	0.806	0.746	0.654
1	LNGP	0.743	0.605	0.639	0.851	0,000	0.795	0.759	0.618
3	1D-LBP	0.827	0.729	0.759	0.886	0.264	0.872	0.812	0.811
3	LNDP	0.792	0.696	0.713	0.857	0.229	0.850	0.811	0.731
3	LGP	0.772	0.659	0.682	0.878	0.126	0.819	0.769	0.701
3	LNGP	0.769	0.638	0.675	0.847	0.067	0.826	0.788	0.662
5	1D-LBP	0.822	0.714	0.750	0.874	0.215	0.87	0.811	0.799
5	LNDP	0.814	0.725	0.742	0.875	0.296	0.866	0.817	0.772
5	LGP	0.776	0.658	0.687	0.850	0.122	0.831	0.766	0.721
5	LNGP	0.784	0.655	0.698	0.875	0.066	0.829	0.783	0.723

Table 5
Performance results for the EOG, as well as various LPT methods and the number of epochs.

N	LPT	*ACC*	*F*1	κ	Per-Class *F*1				
					W	N1	N2	N3	REM
1	1D-LBP	0.753	0.661	0.656	0.824	0.261	0.813	0.695	0.710
1	LNDP	0.708	0.572	0.579	0.781	0.124	0.782	0.507	0.665
1	LGP	0.632	0.474	0.450	0.679	0.008	0.733	0.440	0.511
1	LNGP	0.681	0.536	0.538	0.771	0.000	0.749	0.646	0.513
3	1D-LBP	0.802	0.721	0.725	0.863	0.349	0.844	0.756	0.791
3	LNDP	0.749	0.637	0.639	0.822	0.226	0.804	0.586	0.746
3	LGP	0.647	0.501	0.499	0.654	0.001	0.761	0.557	0.532
3	LNGP	0.709	0.564	0.580	0.776	0,000	0.772	0.692	0.580
5	1D-LBP	0.792	0.703	0.706	0.851	0.334	0.836	0.681	0.812
5	LNDP	0.729	0.606	0.605	0.785	0.177	0.789	0.552	0.727
5	LGP	0.659	0.508	0.511	0.627	0,000	0.781	0.594	0.537
5	LNGP	0.744	0.607	0.636	0.813	0.006	0.788	0.722	0.707

Table 6
Performance results for the Fpz-Cz and Pz-Oz EEGs, as well as various LPT methods and the number of epochs.

N	LPT	*ACC*	*F*1	κ	Per-Class *F*1				
					W	N1	N2	N3	REM
1	1D-LBP	0.832	0.746	0.769	0.902	0.295	0.877	0.852	0.803
1	LNDP	0.812	0.727	0.739	0.880	0.317	0.861	0.812	0.764
1	LGP	0.773	0.654	0.682	0.882	0.117	0.827	0.753	0.694
1	LNGP	0.757	0.628	0.652	0.888	0.108	0.812	0.665	0.666
3	1D-LBP	0.844	0.770	0.785	0.903	0.394	0.876	0.851	0.828
3	LNDP	0.836	0.770	0.772	0.888	0.436	0.875	0.836	0.817
3	LGP	0.800	0.700	0.720	0.866	0.242	0.853	0.794	0.746
3	LNGP	0.754	0.644	0.650	0.872	0.233	0.816	0.596	0.702
5	1D-LBP	0.846	0.769	0.787	0.899	0.365	0.883	0.852	0.848
5	LNDP	0.824	0.739	0.754	0.867	0.338	0.871	0.820	0.799
5	LGP	0.804	0.703	0.723	0.901	0.262	0.849	0.744	0.758
5	LNGP	0.784	0.656	0.693	0.882	0.111	0.829	0.710	0.747

Table 7
Performance results for the Fpz-Cz and Pz-Oz EEGs and EOG, as well as various LPT methods and the number of epochs.

N	LPT	*ACC*	*F*1	κ	Per-Class *F*1				
					W	N1	N2	N3	REM
1	1D-LBP	0.831	0.741	0.762	0.912	0.310	0.866	0.821	0.795
1	LNDP	0.818	0.743	0.747	0.900	0.360	0.862	0.805	0.789
1	LGP	0.778	0.666	0.686	0.870	0.155	0.835	0.772	0.697
1	LNGP	0.773	0.656	0.678	0.892	0.143	0.816	0.728	0.701
3	1D-LBP	0.837	0.748	0.770	0.912	0.317	0.870	0.819	0.821
3	LNDP	0.831	0.759	0.765	0.900	0.394	0.869	0.812	0.819
3	LGP	0.807	0.730	0.728	0.883	0.373	0.849	0.788	0.759
3	LNGP	0.774	0.670	0.679	0.864	0.234	0.819	0.720	0.711
5	1D-LBP	0.848	0.782	0.790	0.897	0.444	0.883	0.849	0.834
5	LNDP	0.836	0.770	0.770	0.891	0.432	0.872	0.821	0.833
5	LGP	0.791	0.706	0.702	0.882	0.312	0.829	0.767	0.742
5	LNGP	0.795	0.678	0.710	0.888	0.148	0.836	0.771	0.746

establish relations between features extracted from successive epochs. LPT methods and models with different numbers of inputs were evaluated on the benchmark Sleep-EDF (version 2013) dataset. We utilized Fpz-Cz EEG, Pz-Oz EEG, and EOG, as well as their combinations. The best performance was obtained using five consecutive epochs of two-channel EEG combined with EOG that were transformed by 1D-LBP. The best overall accuracy, F1 score, and Cohen's kappa coefficients were 0.848, 0.782, and 0.790, respectively.

LPT methods derived from 1D-LBP were introduced to reduce the dependency of 1D-LBP on local variations to some degree. Thus far, these methods and 1D-LBP have been evaluated on relatively easy tasks like epileptic EEG and Parkinson's disease detection using hand-engineered features. Therefore, to evaluate and validate the effectiveness of these methods, we conducted several experiments. Instead of manual feature extraction that might lead to biased results, we used CNNs for feature extraction and classification of sleep stages. To expand their application, LPT methods were applied to EOG in addition to EEG and gait. In the experiments, 1D-LBP consistently outperformed the others regardless of signals or the number of epochs that were employed. Using LNDP instead of 1D-LBP on the Fpz-Oz EEG reduced the best accuracy by 2.7 %, LGP reduced it by 7.6 %, and LNGP reduced it by 8 %. The accuracy differences were much greater in the case of the EOG, with LNDP reducing it by 6.6 %, LGP reducing it by 17.8 %, and LNGP reducing it by 7.8 %. The poor performance of LGP and LNGP compared to 1D-LGP can be explained by the fact that sleep stages are commonly determined by the occurrences of sleep-related events such as sleep spindles, K-complexes, vertex waves, and arousals, which cause transient and local variations in EEG and EOG signals. As a result, reducing their reliance on local differences makes them less ideal for sleep stage scoring task. Finally, an additional experiment was conducted using standardized raw PSG signals (Fpz-Oz and Pz-Oz EEG and EOG) and five successive epochs ($N = 5$) to highlight the value of using LPT (especially 1D-LBP and LNDP) methods, yielding an accuracy of 0.792. This demonstrates the power of 1D-LBP and LNDP to discover hidden patterns in PSG signals.

In the case of per-class F1 scores, the best scores for W, N1, N2, N3, and REM were 0.912, 0.444, 0.883, 0.852, and 0.848, respectively. These results were obtained with 1D-LBP, confirming its superiority over the others once more. In addition, the detection rate was the lowest for N1 because it is the minority class and the transition stage from W to N2, carrying characteristics of both stages. The best scores for W and N1 were obtained when all signals were used, while the rest were achieved using both EEG channels. With the exception of W, the best performances were achieved using models with five inputs.

Fig. 4 depicts overall accuracies for each method and signal, covering all values of N employed during experiments. In terms of the maximum accuracy, 1D-BP performed better with the Fpz-Cz channel compared to Pz-Oz, while there were no significant differences for LNDP and LGP. However, in the case of LNGP, the maximum accuracy was higher with the Pz-Oz. Regardless of the method used, the accuracy of EOG was inferior to other signals and signal combinations, as expected. Nonetheless, 1D-LBP exceeded the accuracy band of 0.8, corroborating the effectiveness of 1D-LBP-based CNN. As a result, considering its ease of use and the convenience it can provide for subjects [46], the EOG can be

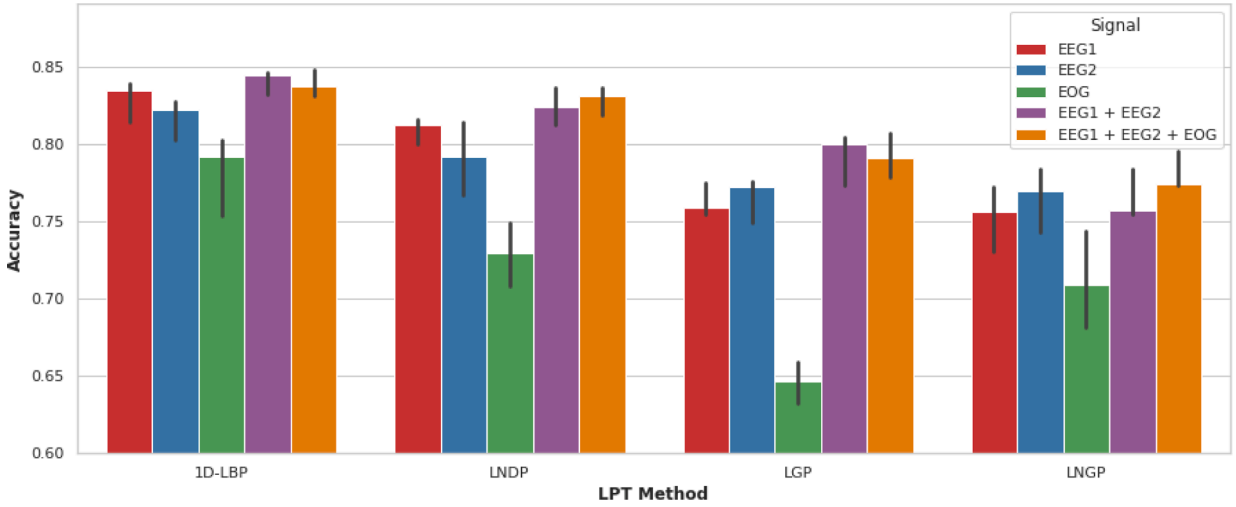

Fig. 4. Bar plot of accuracies for all methods, signals, and values of the number of epochs. Each color represents a signal or signal combination, while each bar indicates the median accuracy for different values of *N*. The vertical line on each bar expands from minimum to maximum accuracy. EEG1 stands for the Fpz-Cz channel, and EEG2 is the Pz-Oz EEG.

considered as a viable alternative to the EEG.

Rechtschaffen and Kales (R&K) guidelines recommended recording at least one channel of central EEG for sleep scoring [47]. The recommendation was based on equipment constraints as well as the opinion that regional variations in scalp areas were not important for sleep stage scoring [48]. The 2007 AASM guideline, on the other hand, advocates using three-channel EEG, which includes frontal, central, and occipital regions. The decision was based on evidence that, whereas sleep spindles are optimally captured from central locations, other sleep-related events such as delta waves, K complexes, and alpha waves are not, and thus the use of single-channel EEG may cause sleep scoring inaccuracies [48]. Our experimental results showed that although frontal-central derivation (Fpz-Cz) outperformed parietal-occipital derivation (Pz-Oz), the fusion of both channels improved the overall accuracies further compared to only Fpz-Oz. Accuracy improvements in 1D-LBP, LNDP, LGP, and LNGP were 0.83 %, 2.45 %, 3.74 %, and 1.55 %, respectively. Improvements were much more limited compared to the fusion of EEG channels when EOG was fused as well. This can be explained by the fact that the EOG conveys only indirect sleep-related events in the form of EEG noise and introduces lots of irrelevant and redundant information that has no or little effect on sleep stage scoring. We concluded that to avoid employing multiple signal types and thus reducing the complexity of the system and enhancing patient convenience during recording, either two-channel EEG or single-channel EOG should be preferred.

The influence of the number of epochs (N) is shown in Fig. 5. In general, the accuracy improved as the number of epochs increased. Regardless of the input signal or signal combination, all methods achieved their maximum accuracies at $N = 3$ or $N = 5$. This pattern was better demonstrated by the average accuracy per number of epochs across all experiments (average lines in Fig. 5). When N was increased from 1 to 5, the average accuracy improved by 2.9 %, 3.1 %, and 5.3 %, respectively, for 1D-LBP, LGP, and LNGP. For LNDP, it was increased by 3.1 % when N was increased from 1 to 3. These results support that employing multiple epochs as input to EpochNet, i.e., blending representative features extracted from multiple successive epochs to classify target epochs, can significantly improve the overall performance.

Table 8 compares the performance of EpochNet to that of state-of-the-art models, including model architectures, PSG signals, deep learning model input types, and the number of epochs concurrently employed for scoring of the target epoch's sleep stage. For fair comparison, studies that did not follow the same experimental procedure were excluded. These methods include the ones that utilize deep learning, the same experimental dataset, and the LOOCV scheme. Our method outperformed all methods, with the exception of XSleepNet2 [42]. EpochNet was designed to be compact and provide both accuracy and speed during training as well as inference, utilizing LPT methods that capture local discriminative patterns from raw PSG signals. We did not utilize RNN or attention since they are slower to train than CNN [49]. EpochNet learns temporal context by blending representative

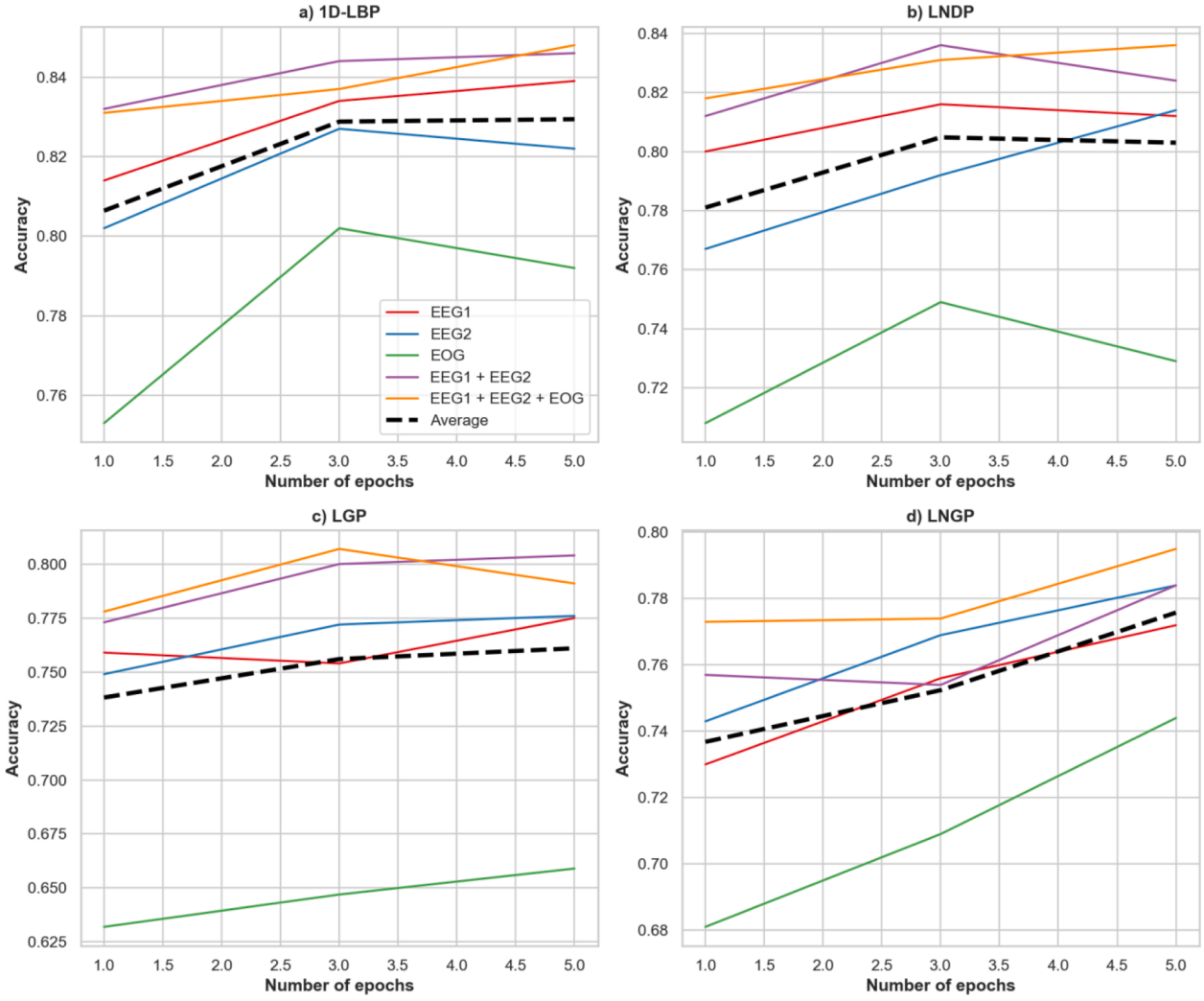

Fig. 5. The accuracy of the proposed approach according to the number of epochs (N). Each graph shows overall accuracy with respect to the number of epochs for each LPT method. Colored lines are for each input type, while the dashed black line is the average of colored lines, which reveals the trend as N increases.

Table 8
Performance comparison between EpochNet and the state-of-the-art methods for automatic sleep scoring via deep learning.

Model	Architecture	PSG Signal	Input Type	# of Epochs	*ACC*	*F*1	κ
EpochNet	CNN	EEG	1D-LBP	5	0.846	0.769	0.79
SleepEEGNet [50]	CNN + RNN	EEG	Raw	All	0.843	0.797	0.79
XSleepNet2 [42]	CNN + RNN	EEG	Raw + Spectrogram	20	**0.863**	**0.806**	**0.813**
IITNet [24]	CNN + RNN	EEG	Raw	10	0.839	0.776	0.78
DeepSleepNet [21]	CNN + RNN	EEG	Raw	All	0.820	0.769	0.76
Phan et al. [26]	Multitask CNN	EEG	Spectrogram	3	0.819	0.738	0.74
Wei et al. [49]	CNN + Attention	EEG	Raw	30	0.843	0.790	0.76
Tsinalis et al. [51]	CNN	EEG	Raw	5	0.748	0.698	0.65
EpochNet	CNN	EEG + EOG	1D-LBP	5	0.848	0.782	0.79
XSleepNet2 [42]	CNN + RNN	EEG + EOG	Raw + Spectrogram	20	**0.864**	**0.809**	**0.813**
Phan et al. [26]	Multitask CNN	EEG + EOG	Spectrogram	3	0.823	0.747	0.75
Andreotti et al. [52]	CNN	EEG + EOG	Raw	1	–	–	0.68
EpochNet	CNN	EOG	1D-LBP	3	**0.802**	**0.721**	**0.72**
Andreotti et al. [52]	CNN	EOG	Raw	1	–	–	0.68
EOGNet [46]	CNN + RNN	EOG	Raw	15	0.763	0.693	0.67

features extracted from multiple successive epochs. Furthermore, EpochNet has few trainable parameters and small convolutional kernels that affect the speed of DNN models. The largest EpochNet has only 0.16×10^6 parameters, while XSleepNet2 has 36 times more parameters and employs 20 epochs of raw data as well as spectrograms. Even though IITNet [24] relies on raw EEG data, it has 3×10^6 trainable parameters, utilizes 10 epochs, and performs slightly worse than EpochNet and XSleepNet2. In general, our approach can achieve comparable performance to other state-of-the-art methods while occupying fewer computing resources. We think the overall performance of sleep stage classification methods can be improved by utilizing LPT methods and more complex DNN models.

6. Conclusion

We have presented a novel framework for sleep stage scoring. The proposed approach employs local pattern transformation methods to transform raw PSG signals into discovered patterns. EpochNet, a CNN model that can accept multiple successive epochs, was used for feature extraction and classification. To evaluate and validate the LPT-based approach, we analyzed four types of LPT methods, including 1D-LBP, LNDP, LGP, and LNGP, different PSG signals and signal combinations, as well as various input sequence length (N). Experimental results showed that 1D-LBP and LNDP-based classification were superior to the other LPT methods, and EpochNet with multiple inputs outperformed single-epoch models. Comparison with state-of-the-art methods demonstrated that the proposed approach can be successfully and efficiently used for sleep stage scoring, obtaining a performance comparable to the other methods.

CRediT authorship contribution statement

Hasan Zan: Methodology, Software, Writing – original draft. **Abdulnasır Yildiz:** Conceptualization, Validation, Writing – review & editing.

Declaration of Competing Interest

The authors declare that they have no known competing financial interests or personal relationships that could have appeared to influence the work reported in this paper.

Data availability

The code used in this article will be published as a separate paper later.

Acknowledgement

The numerical calculations reported in this paper were fully performed at TUBITAK ULAKBIM, High Performance and Grid Computing Center (TRUBA resources).

References

[1] B. Yang, X. Zhu, Y. Liu, H. Liu, A single-channel EEG based automatic sleep stage classification method leveraging deep one-dimensional convolutional neural network and hidden Markov model, Biomed. Signal Process. Control 68 (2021).
[2] S. Ancoli-Israel, L. Ayalon, C. Salzman, Sleep in the elderly: normal variations and common sleep disorders, Harvard Rev. Psychiatry 16 (5) (2008).
[3] K. Wulff, S. Gatti, J.G. Wettstein, R.G. Foster, Sleep and circadian rhythm disruption in psychiatric and neurodegenerative disease, Nat. Rev. Neurosci. 11 (8) (2010) 589–599.
[4] C. Berthomier, X. Drouot, M. Herman-Stoïca, P. Berthomier, J. Prado, D. Bokar-Thire, O. Benoit, J. Mattout, M.-P. d'Ortho, Automatic analysis of single-channel sleep EEG: validation in healthy individuals, Sleep 30 (11) (2007) 1587–1595.
[5] S.S. Kumar, A machine learning model for automated classification of sleep stages using polysomnography signals, in: International Conference on Innovative Computing and Communications. Advances in Intelligent Systems and Computing, Singapore, 2022.
[6] E. Alickovic, A. Subasi, Ensemble SVM method for automatic sleep stage classification, IEEE Trans. Instrum. Meas. 67 (6) (2018) 1258–1265.
[7] E.A. Wolpert, A manual of standardized terminology, techniques and scoring system for sleep stages of human subjects, Arch. Gen. Psychiatry 20 (2) (1969) 246–247.
[8] B. Koley, D. Dey, An ensemble system for automatic sleep stage classification using single channel EEG signal, Comput. Biol. Med. 42 (12) (2012) 1186–1195.
[9] N. Schaltenbrand, R. Lengelle, M. Toussaint, R. Luthringer, G. Carelli, A. Jacqmin, E. Lainey, A. Muzet, J.P. Macher, Sleep stage scoring using the neural network model: comparison between visual and automatic analysis in normal subjects and patients, Sleep 19 (1) (1996) 26–35.
[10] P. Huy, D. Quan, D. The-Luan, V. Duc-Lung, Metric learning for automatic sleep stage classification, in: 2013 35th Annual International Conference of the IEEE Engineering in Medicine and Biology Society (EMBC), Osaka, Japan, 2013.
[11] S. Güneş, K. Polat, Ş. Yosunkaya, Efficient sleep stage recognition system based on EEG signal using k-means clustering based feature weighting, Expert Syst. Appl. 37 (12) (2010) 7922–7928.
[12] T. Lajnef, S. Chaibi, P. Ruby, P.-E. Aguera, J.-B. Eichenlaub, M. Samet, A. Kachouri, K. Jerbi, Learning machines and sleeping brains: automatic sleep stage classification using decision-tree multi-class support vector machines, J. Neurosci. Methods 250 (2015) 94–105.
[13] I. Koprinska, G. Pfurtscheller, D. Flotzinger, Sleep classification in infants by decision tree-based neural networks, Artif. Intell. Med. 8 (4) (1996) 387–401.
[14] Z. Huang, B.-W.-K. Ling, Sleeping stage classification based on joint quaternion valued singular spectrum analysis and ensemble empirical mode decomposition, Biomed. Signal Process. Control 71 (2022), 103086.
[15] A.R. Hassan, M.I.H. Bhuiyan, Computer-aided sleep staging using Complete Ensemble Empirical Mode Decomposition with Adaptive Noise and bootstrap aggregating, Biomed. Signal Process. Control 24 (2016) 1–10.
[16] S.K. Satapathy, A.K. Bhoi, D. Loganathan, B. Khandelwal, P. Barsocchi, Machine learning with ensemble stacking model for automated sleep staging using dual-channel EEG signal, Biomed. Signal Process. Control 69 (2021), 102898.
[17] K. Muhammad, J. Ahmad, Z. Lv, P. Bellavista, P. Yang, S.W. Baik, Efficient deep CNN-based fire detection and localization in video surveillance applications, IEEE Trans. Syst. Man Cybern.: Syst. 49 (7) (2019) 1419–1434.
[18] A. Ullah, J. Ahmad, K. Muhammad, M. Sajjad, S.W. Baik, Action recognition in video sequences using deep bi-directional LSTM with CNN features, IEEE Access 6 (2018) 1155–1166.

[19] M. Sajjad, S. Khan, T. Hussain, K. Muhammad, A.K. Sangaiah, A. Castiglione, C. Esposito, S.W. Baik, CNN-based anti-spoofing two-tier multi-factor authentication system, Pattern Recogn. Lett. 126 (2019) 123–131.
[20] W. Neng, J. Lu, L. Xu, CCRRSleepNet: a hybrid relational inductive biases network for automatic sleep stage classification on raw single-channel EEG, Brain Sciences 11 (4) (2021) 456.
[21] A. Supratak, H. Dong, C. Wu, Y. Guo, DeepSleepNet: a model for automatic sleep stage scoring based on raw single-channel EEG, in: IEEE transactions on neural systems and rehabilitation engineering : a publication of the IEEE Engineering in Medicine and Biology Society, vol. 25, no. 11, 2017, pp. 1998-2008.
[22] A. Sors, S. Bonnet, S. Mirek, L. Vercueil, J.-F. Payen, A convolutional neural network for sleep stage scoring from raw single-channel EEG, Biomed. Signal Process. Control 42 (2018) 107–114.
[23] S. Chambon, M.N. Galtier, P.J. Arnal, G. Wainrib, A. Gramfort, A deep learning architecture for temporal sleep stage classification using multivariate and multimodal time series, IEEE Trans. Neural Syst. Rehabil. Eng. 26 (4) (2018) 758–769.
[24] H. Seo, S. Back, S. Lee, D. Park, T. Kim, K. Lee, Intra- and inter-epoch temporal context network (IITNet) using sub-epoch features for automatic sleep scoring on raw single-channel EEG, Biomed. Signal Process. Control 61 (2020), 102037.
[25] E. Khalili, B. Mohammadzadeh Asl, Automatic sleep stage classification using temporal convolutional neural network and new data augmentation technique from raw single-channel EEG, Comput. Methods Programs Biomed. 204 (2021), 106063.
[26] H. Phan, F. Andreotti, N. Cooray, O.Y. Chen, M. De Vos, Joint classification and prediction CNN framework for automatic sleep stage classification, IEEE Trans. Biomed. Eng. 66 (5) (2019) 1285–1296.
[27] H. Dong, A. Supratak, W. Pan, C. Wu, P.M. Matthews, Y. Guo, Mixed neural network approach for temporal sleep stage classification, IEEE Trans. Neural Syst. Rehabil. Eng. 26 (2) (2018) 324–333.
[28] S. Biswal, J. Kulas, H. Sun, B. Goparaju, M.B. Westover, M.T. Bianchi, J. Sun, SLEEPNET: automated sleep staging system via deep learning, ArXiv, vol. 1707.08262, 2017.
[29] Y.-L. Hsu, Y.-T. Yang, J.-S. Wang, C.-Y. Hsu, Automatic sleep stage recurrent neural classifier using energy features of EEG signals, Neurocomputing 104 (2013) 105–114.
[30] P. Jadhav, G. Rajguru, D. Datta, S. Mukhopadhyay, Automatic sleep stage classification using time–frequency images of CWT and transfer learning using convolution neural network, Biocybern. Biomed. Eng. 40 (1) (2020) 494–504.
[31] Y. Kaya, M. Uyar, R. Tekin, S. Yıldırım, 1D-local binary pattern based feature extraction for classification of epileptic EEG signals, Appl. Math. Comput. 243 (2014) 209–219.
[32] A.K. Jaiswal, H. Banka, Local pattern transformation based feature extraction techniques for classification of epileptic EEG signals, Biomed. Signal Process. Control 34 (2017) 81–92.
[33] Ö.F. Ertuğrul, Y. Kaya, R. Tekin, M.N. Almalı, Detection of Parkinson's disease by Shifted One Dimensional Local Binary Patterns from gait, Expert Syst. Appl. 56 (2016) 156–163.
[34] N.J. Sairamya, S. Thomas George, R. Balakrishnan, M.S.P. Subathra, An effective approach to classify epileptic EEG signal using local neighbor gradient pattern transformation methods, Australas. Phys. Eng. Sci. Med. 41 (4) (2018) 1029–1046.
[35] N.J. Sairamya, S.T. George, D.N. Ponraj, M.S.P. Subathra, Detection of epileptic EEG signal using improved local pattern transformation methods, Circuits Syst. Sig. Process. 37 (12) (2018) 5554–5575.
[36] T.S. Kumar, V. Kanhangad, R.B. Pachori, Classification of seizure and seizure-free EEG signals using local binary patterns, Biomed. Signal Process. Control 15 (1) (2015) 33–40.
[37] S.J. Priya, A.J. Rani, M.S.P. Subathra, M.A. Mohammed, R. Damaševičius, N. Ubendran, Local pattern transformation based feature extraction for recognition of Parkinson's Disease based on gait signals, Diagnostics 11 (8) (2021) 1395.
[38] A.L. Goldberger, L.A.N. Amaral, L. Glass, J.M. Hausdorff, P.C. Ivanov, R.G. Mark, J. E. Mietus, G.B. Moody, C.-K. Peng, H.E. Stanley, PhysioBank, PhysioToolkit, and PhysioNet, Circulation 101 (23) (2000).
[39] R.B. Berry, R. Brooks, C. Gamaldo, S.M. Harding, R.M. Lloyd, S.F. Quan, M. T. Troester, B.V. Vaughn, AASM Scoring Manual Updates for 2017 (Version 2.4), J. Clin. Sleep Med. 13 (05) (2017) 665–666.
[40] N. Chatlani, J.J. Soraghan, Local binary patterns for 1-D signal processing, in: 18th European Signal Processing Conference, Aalborg, 2010.
[41] M. Lin, Q. Chen, S. Yan, Network in network, arXiv preprint arXiv, vol. 1312.4400, 2013.
[42] H. Phan, O.Y. Chen, M.C. Tran, P. Koch, A. Mertins, M. De Vos, XSleepNet: multi-view sequential model for automatic sleep staging, IEEE Trans. Pattern Anal. Mach. Intell. (2021) 1.
[43] D.P. Kingma, J. Ba, Adam: a method for stochastic optimization, arXiv, vol. 1412.6980, 2014.
[44] M. Abadi, A. Agarwal, P. Barham, E. Brevdo, Z. Chen, TensorFlow: large-scale machine learning on heterogeneous distributed systems, arXiv Preprint 1603 (2016) 04467.
[45] R.M. Schmidt, F. Schneider, P. Hennig, Descending through a Crowded Valley - Benchmarking Deep Learning Optimizers, arXiv 2007 (2020) 01547.
[46] J. Fan, C. Sun, M. Long, C. Chen, W. Chen, EOGNET: a novel deep learning model for sleep stage classification based on single-channel EOG signal, Front. Neurosci. 15 (2021).
[47] A. Rechtschaffen, A manual for standardized terminology, techniques and scoring system for sleep stages in human subjects, Brain Information Service (1968).
[48] W.R. Ruehland, F.J. O'Donoghue, R.J. Pierce, A.T. Thornton, P. Singh, J. M. Copland, B. Stevens, P.D. Rochford, The 2007 AASM recommendations for EEG electrode placement in polysomnography: impact on sleep and cortical arousal scoring, Sleep 34 (1) (2011) 73–81.
[49] W. Qu, Z. Wang, H. Hong, Z. Chi, D.D. Feng, R. Grunstein, C. Gordon, A residual based attention model for EEG based sleep staging, IEEE J. Biomed. Health. Inf. 24 (10) (2020) 2833–2843.
[50] S. Mousavi, F. Afghah, U.R. Acharya, SleepEEGNet: automated sleep stage scoring with sequence to sequence deep learning approach, PLoS ONE 14 (5) (2019), e0216456.
[51] O. Tsinalis, P.M. Matthews, Y. Guo, Automatic sleep stage scoring using time-frequency analysis and stacked sparse autoencoders, Ann. Biomed. Eng. 44 (5) (2016) 1587–1597.
[52] F. Andreotti, H. Phan, N. Cooray, C. Lo, M. T. M. Hu, M. De Vos, Multichannel Sleep Stage Classification and Transfer Learning using Convolutional Neural Networks, in: 2018 40th Annual International Conference of the IEEE Engineering in Medicine and Biology Society (EMBC), Honolulu, HI, USA, 2018.